RPN53

HIGH ν/γ ELECTRON BEAM GENERATION USING A 100 kV MYLAR STRIPLINE

PIIR-4-71

by
G. Loda and P. Spence

November 1970

Physics International Company
2700 Merced Street
San Leandro, California 94577

CONTENTS

ILLUSTRATIONS

SECTION 1

INTRODUCTION

This paper will describe electron beam generation and control on a 100-kV Mylar stripline generator, constructed for DASA by Physics International Company (Reference 1). With this machine, beams of $v/\gamma > 25$ can be produced at the anode window. Results presented include both measurement and analysis of diode impedance collapse, assuming an exploding anode and comparison of beam pinching in the diode with predictions of Friedlander and Jory (Reference 2). The result to be emphasized on beam propagation is a negative one; that is, while we have had beams of $v/\gamma > 25$ at the anode, the propagation of these beams in a neutral gas for more than a few centimeters has been found impossible.

SECTION 2

STRIPLINE GENERATOR

A schematic representation of the machine is given in Figure 1. It consists of two 0.6-ohm Blumleins, in parallel, feeding a variable-impedance field-emission cathode through a low-inductance tube geometry. A two-stage Marx generator is

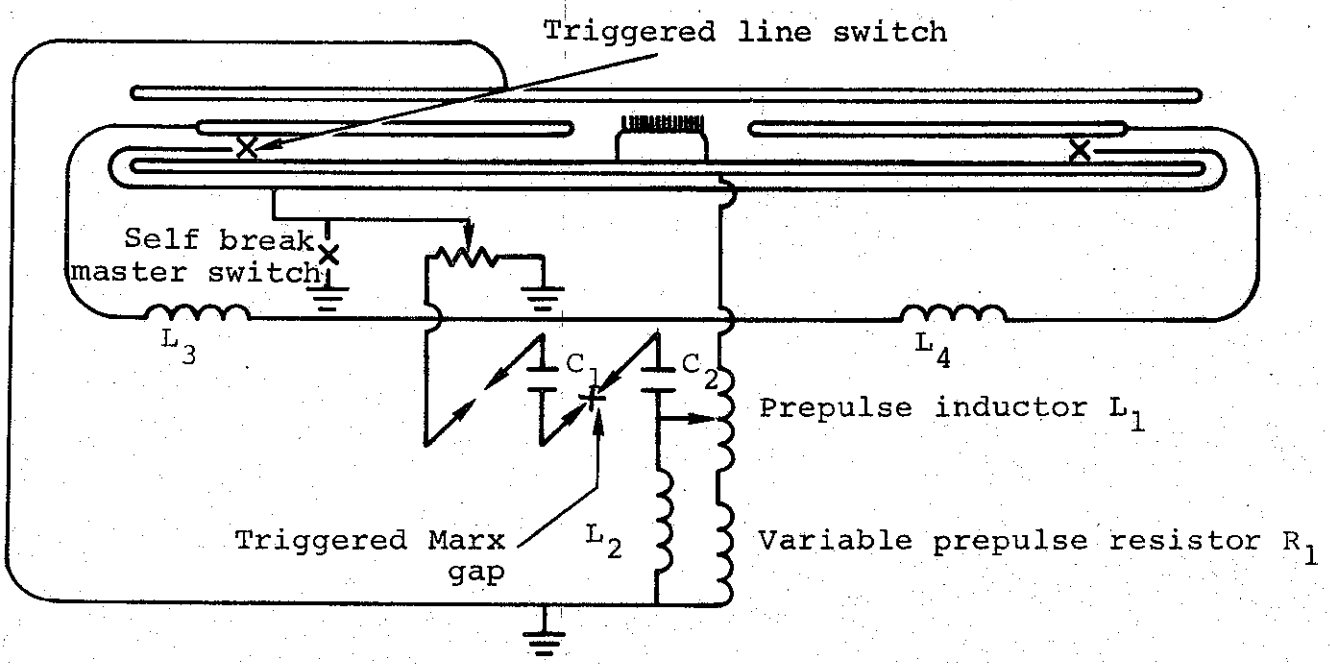

Figure 1 Schematic representation of generator.

used to pulse charge the two Blumleins on a microsecond time scale. When the desired charge is reached, a self-breaking master switch is overvolted, resulting in the triggering of the four solid dielectric line switches. These switches fire with nanosecond jitter allowing a fast-rising wave to be applied to the diode. The inductance of the switches requires two switches to be used in each line to keep the L/R risetime $\leqslant$ 20 nsec.

The entire stripline-tube assembly is immersed in a water-$CuSO_4$ solution:

a. The water (ε = 81) serves to clamp the electric field in the very high dielectric strength Mylar (E = 1.6×10^6 volts/cm, ε = 2.7).

b. The $CuSO_4$ resistively grades any sharp edges on the stripline, resulting in a smearing of the potential so as not to exceed the dielectric strength of the water.

Prepulse* can be adjusted to less than one percent of the main pulse amplitude to eliminate any effect on diode behavior. When operating into a matched load (0.3 ohm), an electron pulse of 100-keV mean energy, 300 kA peak current, and a FWHM duration of 40 nsec is produced.

Fast diagnostics ($\geqslant$ 250 MHz) allowed accurate measurements to be made of both the diode and beam behavior. Shown in Figure 2 are the current monitor [a self-integrating magnetic fluxmeter (Rogowski coil) surrounding the cathode] and the capacitive voltage monitor. To obtain the true voltage across the anode-cathode gap, a component due to the inductance of the cathode

*Prepulse is defined here to be any field present in the anode-cathode gap during the charging cycle and before switching of the Blumlein into the load.

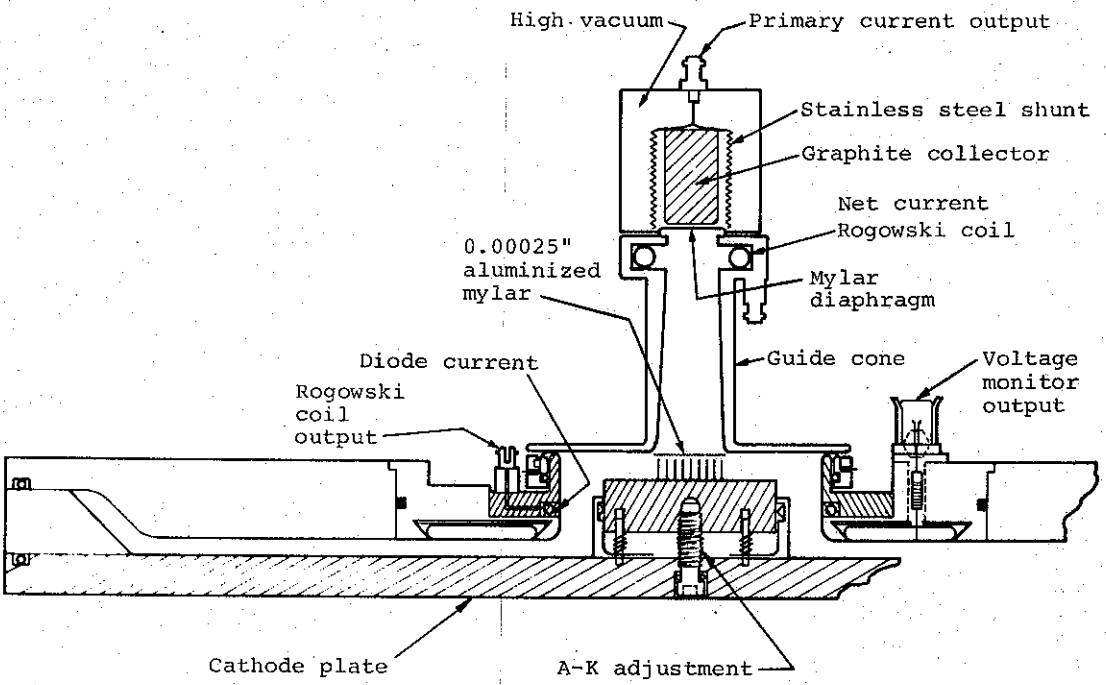

Figure 2 Diode and drift chamber diagnostics.

must be subtracted. This usually amounts to $\leq$10 percent of the measured voltage. Also shown are the drift chamber diagnostics, consisting of the net current monitor (Rogowski coil) and primary current monitor (Faraday cup). Calibrated adjustment of the anode-cathode spacing was possible while the tube was under vacuum with a differential pressure across the anode.

SECTION 3

DIODE IMPEDANCE

Diode impedance on machines of this type has generally been described by a Child's Law behavior:

$$Z = \frac{136}{V^{\frac{1}{2}}} \frac{d^2}{r^2}$$

with the Child's Law constant allowed to vary from its calculated value of 136 down to 60 or 70. We found, however, that with our small anode-cathode gaps of 1 to 2 millimeters, a single impedance value could not be determined. That is, the impedance changed continuously throughout the pulse. We have attempted to analyze this behavior in the following simple model.

After a short time (10 nsec), the anode is assumed to consist of a highly conductive plasma, exploding from its midplane at a velocity of 1.5 cm/sec. This explosion is the thermo-mechanical response of the anode to the high energy density loading of the electron beam. An anode velocity such as this is consistent with framing camera data taken on other e-beam machines at similar dose levels. Figure 3 shows the remarkable fit to the data that this model gives. The solid lines are the calculated impedance values, while the points are the actual data, with the error bars indicating an average of three shots.

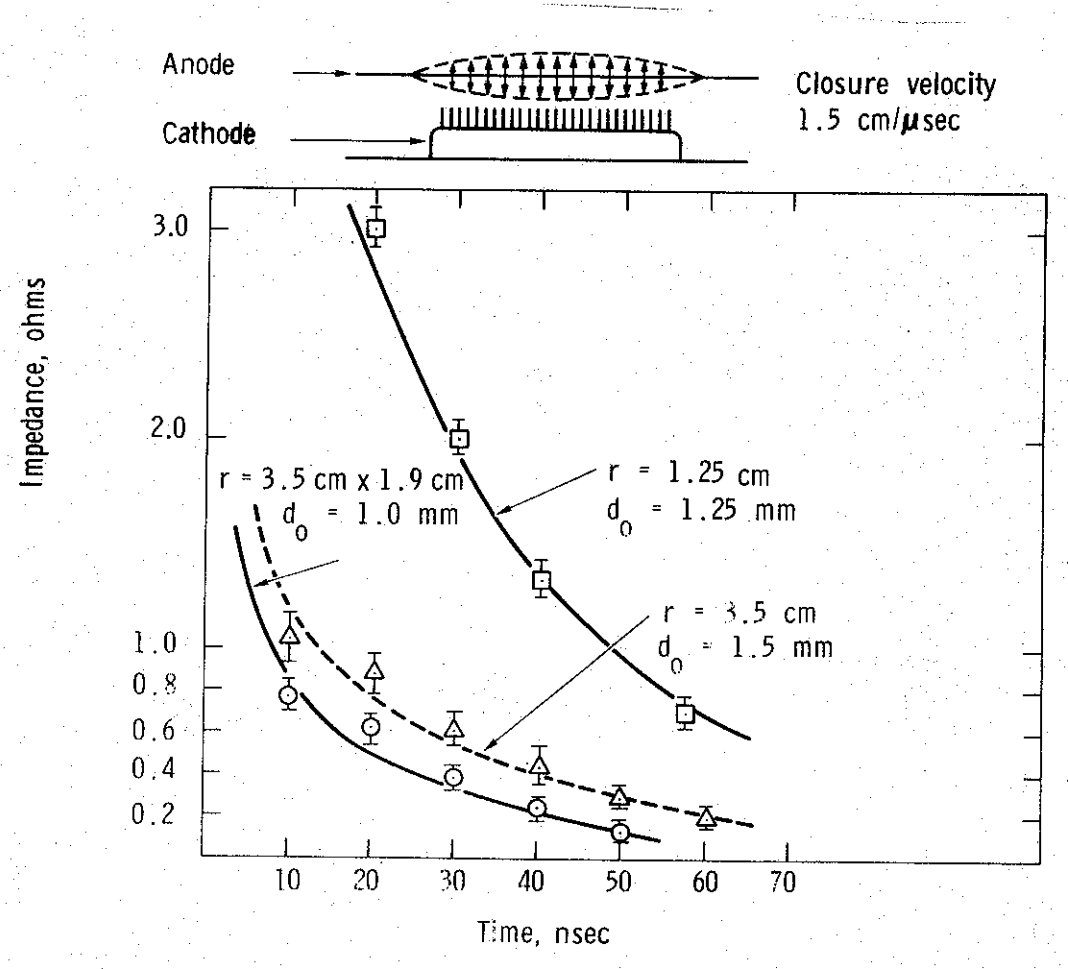

Figure 3 Diode impedance.

Child's Law

$$Z = \frac{136}{V^{\frac{1}{2}}} \frac{d^2}{r^2}$$

$$d = d_o - v(t-10)$$

V in megavolts, t in nsec

r = Cathode radius

Pinching of the electron-beam in the anode-cathode gap has long been observed on high-current machiens of this type. An insight into this phenomena has been given by Friedlander and Jory (Reference 2). Their model shows that pinching of the beam will begin when the diode current is equal to I_C, which is the value of the current where the Larmor radius for an electron emitted from the edge of the cathode is equal to the anode-cathode spacing. This critical current is

$$I_C \text{ (amps)} = 8500\ \beta\gamma\ (r/d)$$

where

r = cathode radius

d = anode-cathode spacing

$\gamma = (1-\beta^2)^{-\frac{1}{2}}$

This model assumes that there is no space-charge neutralization in the diode (i.e., positive ions are not present). It gives no information as to the velocity of the pinch collapse or the current distribution at the anode during the pinch. Present analytical methods have not provided the answer to these important questions.

An experiment was undertaken to determine $J(r,t)$ at the anode plane. A series of shots were taken using an apertured Faraday cup as an anode. Then, by normalizing each shot to a fixed total diode current, $J(r,t)$ was obtained. The results of this work are shown in Figure 4. The hollow-beam picture presented is subject to question. There are at least two experimental difficulties in determining $J(r,t)$ at small r:

a. An off-axis formation of the beam pinch, including a "wandering" of the beam during the pulse

b. A masking of the large-angle components of the beam due to the finite thickness of the aperture.

Within these limitations, a good picture has been obtained of the time history of the pinch.

Figure 4 gives a plot of the critical current versus time and the measured diode current for a typical shot. (The critical current is time-dependent due to both the changing diode voltage and the velocity of the exploding anode.) The time at which pinching begins, predicted by the model to be at 32 nsec, is in reasonable agreement with the J(r,t) measurement shown in the upper half of Figure 4.

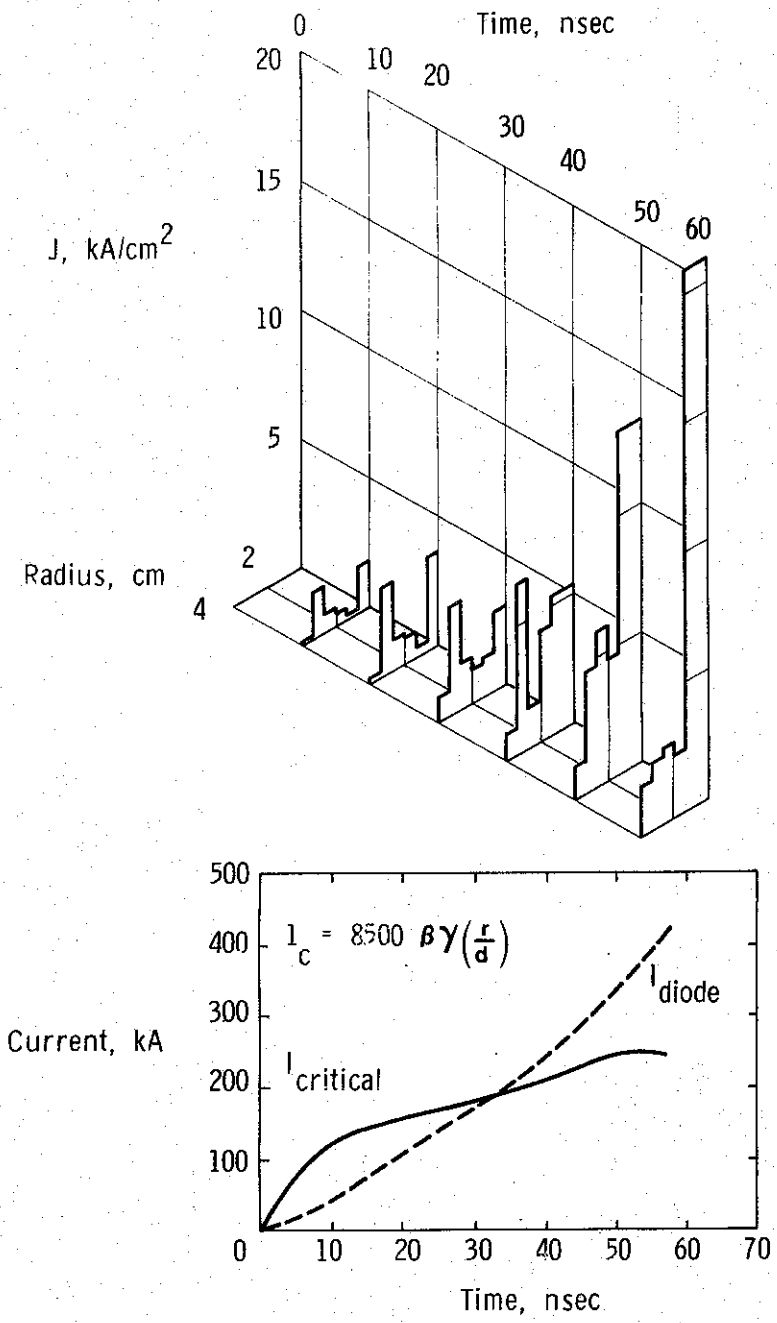

Figure 4 Diode pinching.

SECTION 4

BEAM TRANSPORT

As stated previously, it was found impossible to transport in a neutral gas the very high ν/γ beams that this machine can produce. This can be attributed to the inability of the self-magnetic field of the beam to contain the transverse energy of the beam and to simultaneously maintain a low enough dI_{net}/dt so as not to stop the beam because of its own back emf. Lower ν/γ beams, on the order of 1 to 4, have been readily produced by turning down the machine output somewhat. Figure 5 shows an example of such a beam. The voltage trace shown in the first graph has been corrected for the inductive drop across the cathode structure. The second graph represents the primary electron current, measured by the Faraday cup at the end of the guide pipe, and the net current (primary current minus the plasma current) measured just prior to the Faraday cup. The bottom represents the ratio of transverse energy to longitudinal energy of the electron beam calculated from the magnetic-pressure-balance relation shown (Reference 3). A check on both this pressure-balance relation and on the diagnostics has been performed by taking a series of number transmission measurements in aluminum and then performing Monte Carlo calculations of electron transport that used diagnostic traces and the pressure-balance relation as imput. These data are shown in Figure 6.

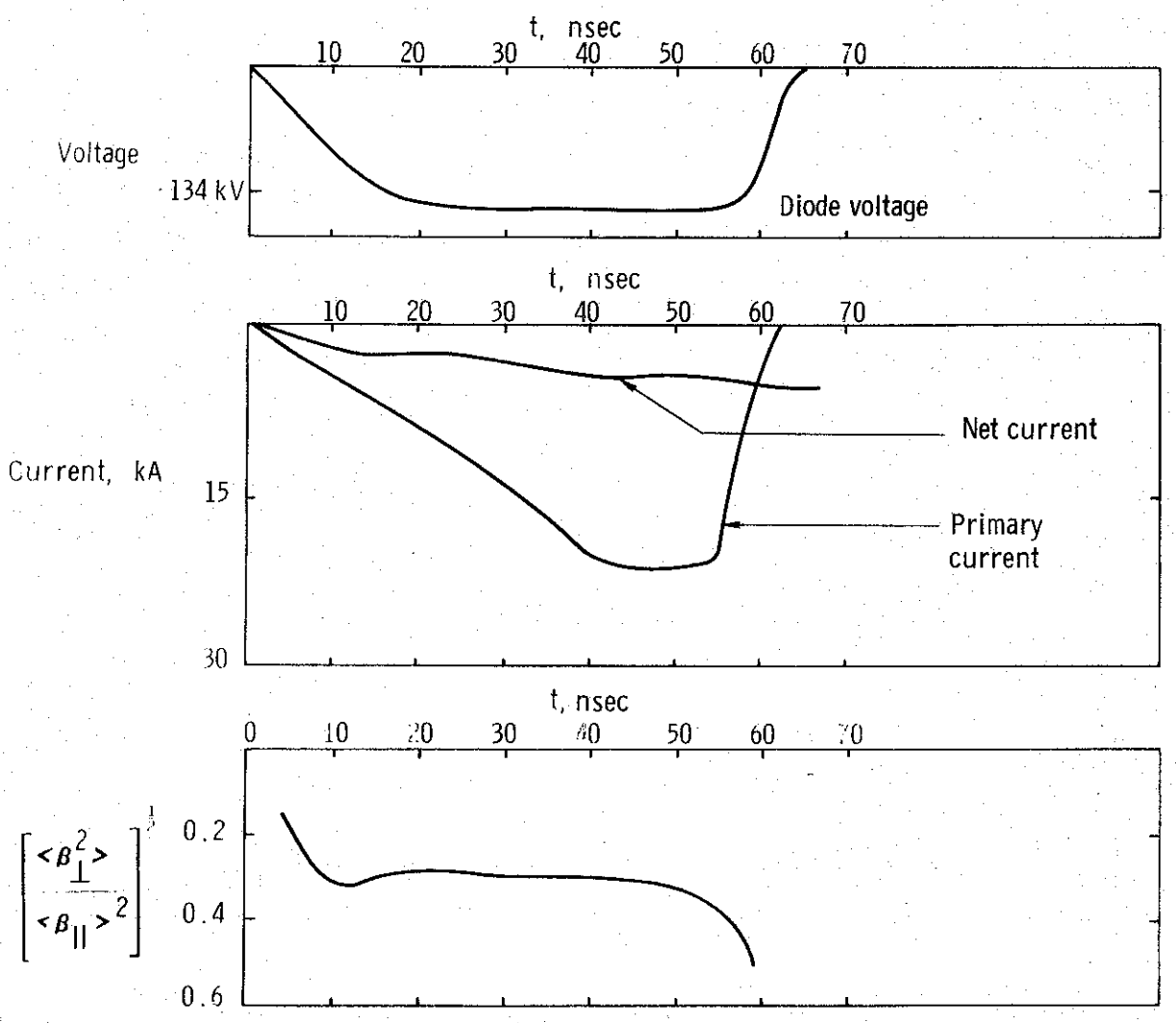

$$\frac{\langle\beta_\perp^2\rangle}{\langle\beta_\parallel\rangle^2} = \frac{\nu}{\gamma}\ (1 - f_m)^2$$

$$\text{where } \nu = \frac{I_{pri}}{17000}\ \frac{1}{\langle\beta_\parallel\rangle}$$

Figure 5 Beam transport in 0.9 torr air.

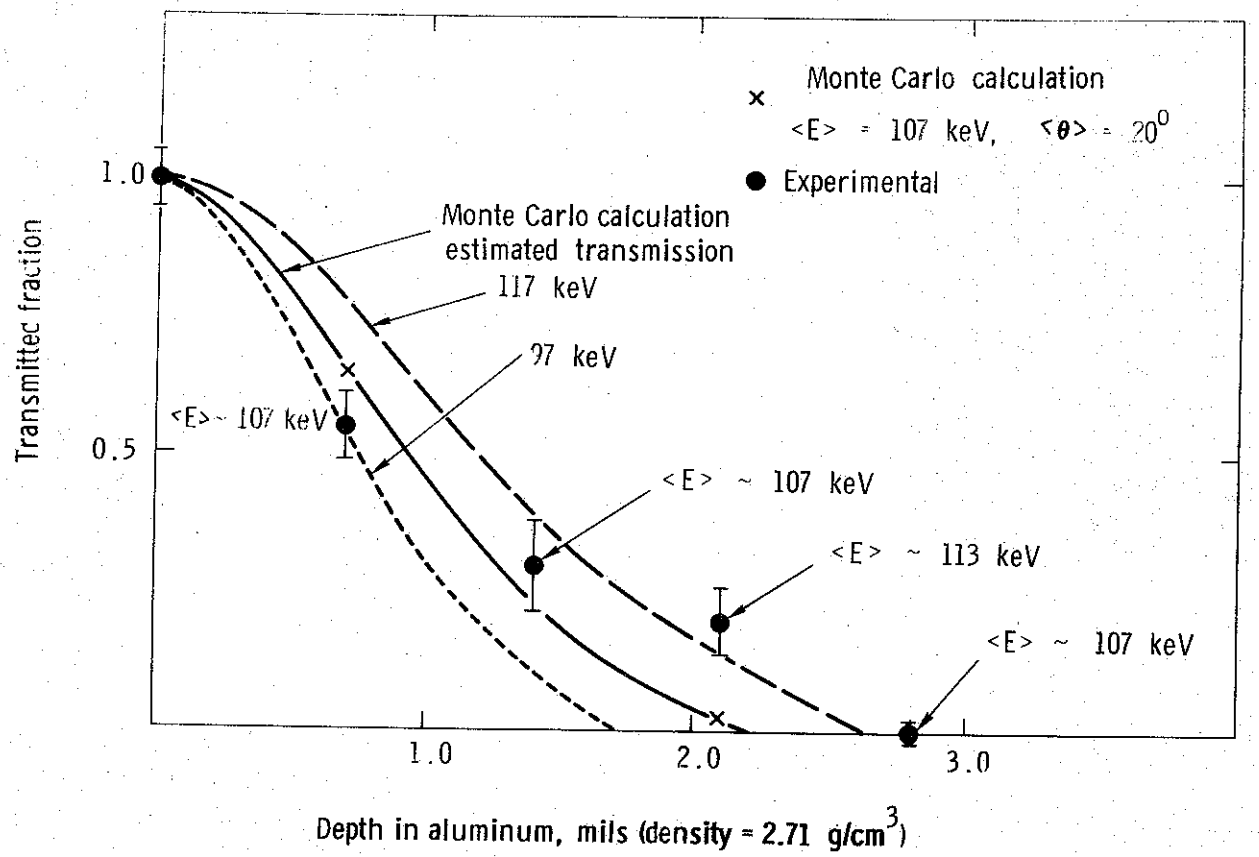

Figure 6 Electron number transmission through aluminum filters.

SECTION 5
CONCLUSIONS

Diode impedance and impedance collapse can be predicted with a modified Child's Law behavior. Pinching of the electron beam in the diode has been observed and is in reasonable agreement with the predictions of Friedlander and Jory. Beams with the kinetic energy and current levels produced by this machine cannot be propagated efficiently in a neutral gas. They can, however be propagated in preionized gas and external magnetic fields (Reference 4).

REFERENCES

1. I. Smith, et al., DASA 2482, August 1970.

2. F. Friedlander, "Megavolt-Megampere Electron Gun Study," Varian Associates Report, 1968.

3. G. Yonas, et al., DASA 2426, August 1969.

4. C. Stallings, "High ν/γ Electron Beam Transport in Preionized B_z Field," PIIR-24-70, Physics International Company, San Leandro, California, October 1970. Presented at November APS meeting, Washington, D. C.